

AD-A218 944

WRDC-TR-90-2011

DTIC FULL COPY

①

SUPERCONDUCTING PERMANENT MAGNETS



Stefan L. Wipf
Henry L. Laquer

CryoPower Associates
P.O. Box 478
Los Alamos, NM 87544-0478

March 1990

Final Report for Period June 1987 - August 1988

Approved for Public Release; Distribution is Unlimited

AERO PROPULSION AND POWER LABORATORY
WRIGHT RESEARCH AND DEVELOPMENT CENTER
AIR FORCE SYSTEMS COMMAND
WRIGHT-PATTERSON AIR FORCE BASE, OHIO 45433-6563

DTIC
ELECTE
MAR 2 1990
S B D

90 03 01 223

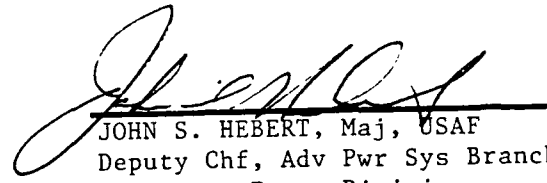
NOTICE

When Government drawings, specifications, or other data are used for any purpose other than in connection with a definitely Government-related procurement, the United States Government incurs no responsibility or any obligation whatsoever. The fact that the government may have formulated or in any way supplied the said drawings, specifications, or other data, is not to be regarded by implication, or otherwise in any manner construed, as licensing the holder, or any other person or corporation; or as conveying any rights or permission to manufacture, use, or sell any patented invention that may in any way be related thereto.

This report is releasable to the National Technical Information Service (NTIS). At NTIS, it will be available to the general public, including foreign nations.

This technical report has been reviewed and is approved for publication.


JAM, Advanced Power Systems Branch
Aerospace Power Division
Aero Propulsion and Power Laboratory


JOHN S. HEBERT, Maj, USAF
Deputy Chf, Adv Pwr Sys Branch
Aerospace Power Division
Aero Propulsion and Power Laboratory

FOR THE COMMANDER


MICHAEL D. BRAYNICH, Maj, USAF
Deputy Director
Aerospace Power Division
Aero Propulsion & Power Laboratory

If your address has changed, if you wish to be removed from our mailing list, or if the addressee is no longer employed by your organization please notify WRDC/POOX, WPAFB, OH 45433-6563 to help us maintain a current mailing list.

Copies of this report should not be returned unless return is required by security considerations, contractual obligations, or notice on a specific document.

REPORT DOCUMENTATION PAGE

Form Approved
OMB No. 0704-0188

1a. REPORT SECURITY CLASSIFICATION UNCLASSIFIED		1b. RESTRICTIVE MARKINGS	
2a. SECURITY CLASSIFICATION AUTHORITY		3. DISTRIBUTION / AVAILABILITY OF REPORT Approved for Public release; Distribution is Unlimited.	
2b. DECLASSIFICATION / DOWNGRADING SCHEDULE			
4. PERFORMING ORGANIZATION REPORT NUMBER(S) cPi TR-88-01b cPi TR-88-02		5. MONITORING ORGANIZATION REPORT NUMBER(S) WRDC-TR-90-2011	
6a. NAME OF PERFORMING ORGANIZATION CryoPower Associates	6b. OFFICE SYMBOL (If applicable)	7a. NAME OF MONITORING ORGANIZATION Wright Research and Development Center Aero Propulsion and Power Laboratory	
6c. ADDRESS (City, State, and ZIP Code) P.O. Box 478 Los Alamos, NM 87544-0478		7b. ADDRESS (City, State, and ZIP Code) WRDC/POOX Wright-Patterson Air Force Base, OH 45433-6563	
8a. NAME OF FUNDING / SPONSORING ORGANIZATION Advanced Power Systems Branch	8b. OFFICE SYMBOL (If applicable) WRDC/POOX-3	9. PROCUREMENT INSTRUMENT IDENTIFICATION NUMBER F33615-87-C-2747	
8c. ADDRESS (City, State, and ZIP Code) Wright Research and Development Center Wright-Patterson AFB, OH 45433-6563		10. SOURCE OF FUNDING NUMBERS	
		PROGRAM ELEMENT NO. 63221C	TASK NO. 0007
		PROJECT NO. D822	WORK UNIT ACCESSION NO.
11. TITLE (Include Security Classification) Superconducting Permanent Magnets			
12. PERSONAL AUTHOR(S) Stefan L. Wipf and Kenry L. Laquer			
13a. TYPE OF REPORT Final	13b. TIME COVERED FROM 6/87 TO 8/88	14. DATE OF REPORT (Year, Month, Day) 1990 March	15. PAGE COUNT 24
16. SUPPLEMENTARY NOTATION			
17. COSATI CODES		18. SUBJECT TERMS (Continue on reverse if necessary and identify by block number)	
FIELD	GROUP	SUB-GROUP	
22	02	High Temperature Superconductors	
10	03	Superconducting Permanent Magnets	
		Superconducting Oxides	
19. ABSTRACT (Continue on reverse if necessary and identify by block number) Superconductors at elevated temperatures will be much less susceptible to thermal instabilities than the classical superconductors at liquid helium temperatures. This is a consequence of the increased specific heat of all materials at elevated temperatures, and removes the need for the extremely fine degree of subdivision exemplified by present state-of-the-art copper stabilized multifilamentary superconducting composites. It should thus be possible to use simple monolithic high temperature superconducting structures, without direct connections to an external power source, to trap fields of at least 3 T at 77 K and thereby produce superconducting permanent magnets with energy products of 225 MG·Oe. The application of high temperature superconductors would be eased and expedited by removing the problems associated with current connections to ordinary conductors and, at the same time, eliminating the heat leak and refrigeration costs associated with current leads between ambient and cryogenic temperatures. The findings of this SBIR Phase I effort are contained in two papers: "Stability Projections for High Temperature Superconductors"			
20. DISTRIBUTION / AVAILABILITY OF ABSTRACT <input checked="" type="checkbox"/> UNCLASSIFIED/UNLIMITED <input type="checkbox"/> SAME AS RPT. <input type="checkbox"/> DTIC USERS		21. ABSTRACT SECURITY CLASSIFICATION UNCLASSIFIED	
22a. NAME OF RESPONSIBLE INDIVIDUAL JERRELL M. TURNER		22b. TELEPHONE (Include Area Code) (513) 255-5179	22c. OFFICE SYMBOL WRDC/POOX-3

UNCLASSIFIED

19. Abstract (Contd)
and "Superconducting Permanent Magnets".

Accession For	
NTIS GRA&I	<input checked="" type="checkbox"/>
DTIC TAB	<input type="checkbox"/>
Unannounced	<input type="checkbox"/>
Justification	
By _____	
Distribution/	
Availability Codes	
Dist	Avail end/or Special
A-1	



Superconducting Permanent Magnets

by

Stefan L. Wipf and Henry L. Laquer

Abstract

The concept of superconducting "permanent" magnets or Super-Permanent magnets, with fields trapped in shells or cylinders of type II superconductors is an old one. Unfortunately, the low values of 0.5 to 1T for the first flux jump field, which is independent of the actual current density, have frustrated its implementation with the classical Type II superconductors. The fact that the flux jump fields for high temperature superconductors should be almost an order of magnitude larger at liquid nitrogen temperatures, allows us to reconsider these options. Analysis of the hysteresis patterns, based on the critical state model, shows that, if the dimensions are chosen so that the sample is penetrated at a field B_p , which is equal to, or just less than the value of the first flux jump field $B_{\epsilon j}$ at the given operating temperature, a temporarily applied field of $2 B_{\epsilon j}$ will trap $0.5 B_{\epsilon j}$. Thus for a $B_{\epsilon j}$ of 6 T, a permanent field of 3 T should be trapped, with an energy product of 1.8 MJ/m^3 (225 MG-Oe). This is five times as large as for the best permanent magnet materials. We discuss means to verify the analysis and the limitations imposed by the low critical current densities in presently available high temperature superconductors.

1. Introduction

The idea of superconducting "permanent" magnets or SuperPermanent magnets, with fields trapped in shells or cylinders of type II superconductors is an old one. It probably occurred to many people and was indeed demonstrated by one of the authors in 1963. [1] The practical implementation of the concept, however, was limited at the time by the low flux jump fields encountered with massive type II specimens, such as Nb_3Sn , Fig. 1, and, more importantly, by the thermal and mechanical consequences of a flux jump, which could be disastrous, Fig. 2. The advent of high temperature superconductors suggests a reexamination of the practicality of superconducting permanent magnets for two reasons:

- o Expected flux jump fields are at least an order of magnitude larger than in previously known type II superconductors, and
- o Higher operating temperatures present an easier and simpler environment for most engineering applications.

Additional motives for wanting to replace solenoidally wound electromagnets with flux trapping structures are to:

- o Bypass many of the difficulties associated with fabricating brittle materials into wire, cable or tape, and
- o Avoid making current carrying contacts between normal conductors and superconductors.

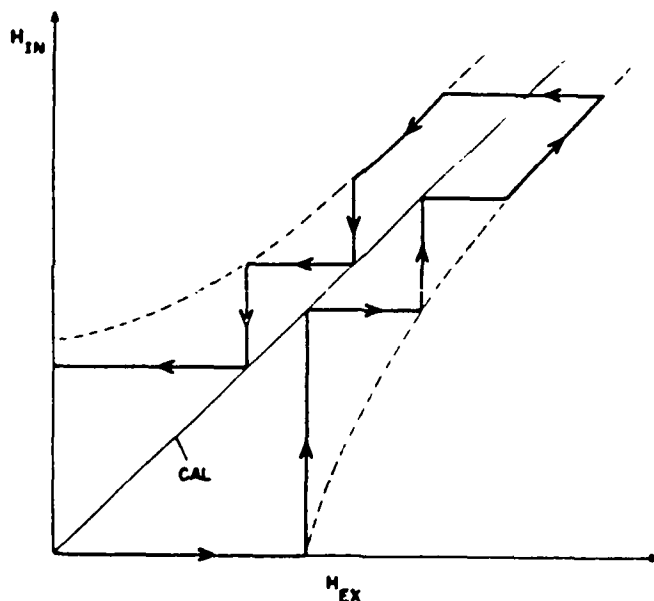


Fig. 1 Flux Trapping with Nb_3Sn cylinder at 4 K.

The steps are flux jumps due to thermal instabilities. The residual internal field, H_{IN} , at zero applied field, H_{EX} , is the trapped or remanent field.



Fig. 2 Nb_3Sn Flux Trapping Cylinder: (a) Before and (b) After Flux Jump.

2. Flux Jumps

2.1. Flux Penetration Mechanisms

It was observed early in the development and application of type II superconductors that heavy walled cylinders, thick sections and wide tapes exhibit a peculiar instability associated with the sudden re-distribution of magnetic fields. The understanding, explanation and avoidance of the interacting thermal, magnetic and uniquely superconducting effects that cause flux jumps have been the primary accomplishments that make large superconducting systems possible. The topic is generally referred to as the adiabatic stability theory, because the worst-possible condition of a thermally isolated system is assumed. In actual practice, it is possible to exceed the predicted adiabatic limits by controlling the rate of flux motion or by changing the structure, so that the assumption of adiabaticity is no longer valid. Nevertheless, the theory provides a sound basis to guarantee engineering reliability.

In describing the electromagnetic characteristics of bulk Type II superconductors, we have to distinguish between the intrinsic properties of ideal materials and the actual behavior of practical ones. When a field is first applied to the ideal material, the field is excluded from the body by currents flowing only in a London surface penetration layer, just as it is in a Type I superconductor. We also observe the Meissner effect, which is the complete expulsion of flux from the superconducting body, when it is cooled in a small static field to below its transition temperature. In either case, the process is energetically demanding and requires that the thermodynamic free energy difference between the normal and superconducting states be larger than the energy of the excluded field. The induction, B , is zero, the magnetization, $M = B - \mu_0 H$, is negative, the relative permeability is -1, and diamagnetism is complete.

The difference between Type I and Type II materials is that when the field exceeds a critical value H_c , Type I loses superconductivity altogether, whereas in Type II flux starts to penetrate the bulk at, what is now designated as the "lower critical field", H_{c1} or B_{c1} . With further increases in H , more field penetrates the Type II, diamagnetism becomes partial and continues to decrease until it finally disappears, together with bulk superconductivity, at the "upper critical field", B_{c2} . In hard-to-achieve ideal samples, the magnetization curve is reversible and retraces when the applied field is decreased.

In practical, non-ideal Type II superconductors the magnetization curves are no longer reversible. Currents throughout the body are governed by the pinning strength, *i.e.* by the ability of various lattice imperfections to pin flux lines and keep them from moving. The situation is described by the Bean-London [2] [3] critical state model. The superconductor initially excludes the magnetic field from its interior by setting up shielding currents on its surface. Once the induced currents exceed what can be carried within the London penetration depth, current gradually transfers into the interior. Local current densities are either at their critical value, behind the moving boundary, or zero, in front of it. The apparent diamagnetism continues to increase for some region above H_{C1} , but at a lower rate than initially. When the field is reversed, there is hysteresis and we may observe an apparent paramagnetism, whenever the average field in the superconductor exceeds the external field during the down-sweep. The Bean-London model is also used to analyze AC losses.

It is important to emphasize that, in materials that pin flux lines, there can be little flux expulsion and most of the observed flux exclusion does not result from the thermodynamically reversible Meissner effect, but merely from shielding by induced currents, as would be seen with any perfect conductor of zero resistivity located in a changing magnetic field.

The original treatment of adiabatic stability was presented in a set of papers by Peter Smith's group at the Rutherford Laboratory [4] and is summarized in Martin Wilson's book "Superconducting Magnets". [5] The theory uses the Bean-London model to quantitatively discuss the energy deposition within the superconductor while exposed to a changing magnetic field. As flux and current progress into the superconducting body, a magnetic field gradient is established. The field drops from the externally applied value to zero at the flux penetration boundary. Eventually, the superconductor will be completely penetrated by magnetic flux and currents when the boundary meets another surface or another boundary coming in from the opposite direction, unless there is a sudden, premature, catastrophic flux motion or flux jump. The jump releases the energy stored in the inductance associated with the shielding currents (*i.e.* the associated magnetic fields gradients), and is therefore always accompanied by local heating. After the flux jump, flux and current distributions are random and unpredictable.

Flux jumps are a consequence of the facts that:

- 1) flux motion in any conductor is a dissipative process and, therefore, releases heat,
- 2) the critical current density in most superconductors decreases with increasing temperature,
- 3) the specific heat of all solids is very low at liquid helium temperatures, so that a small heat input causes a large increase in temperature, and
- 4) the thermal conductivity of most superconductors is low, so that thermal conditions are locally adiabatic.

Flux jumps can be avoided by limiting the dimensions of the superconductor (in the direction perpendicular to any changing field), so that it will be fully penetrated before the field at the surface reaches a critical value, designated as B_{fj} .

2.2. Adiabatic Stability Theory

The following analysis treats a semi-infinite slab of superconductor with a field parallel to its surface. The conductor is assumed to be at a uniform temperature, *i.e.* isothermal, but it is also assumed to be thermally isolated, so that the process will be adiabatic. We then consider a "feedback" cycle where:

A small heat input causes an increase in temperature, T , which causes a decrease in critical current density, J_c , which then results in a redistribution of the shielding currents and thus changes the flux distribution. This flux motion, in turn, produces additional heating.

Depending on the magnitude of the specific heat and of the slope of the critical current density vs. temperature curve, the cycle will either accelerate or die out.

If we make the simplifying assumption that the critical current density, J_c , is independent of the local magnetic field, the flux penetration depth, a , at any time, will be directly proportional to the applied field, B , and inversely to the critical current density, J_c :

$$a = B/(\mu_0 J_c) . \quad (1)$$

The thermal run-away or flux jumping instability criterion is

$$B_{fj} = \left[3 \mu_0 \gamma C \cdot [J_c / (-\partial J_c / \partial T)] \right]^{0.5}, \quad (2)$$

where:

- γ = Density,
- C = Heat capacity per unit mass, and
- γC = Volumetric heat capacity.

We also assume that the critical current density falls linearly with increasing temperature, as observed with most Type II superconductors:

$$-\partial J_c / \partial T = -J_0 / (T^* - T_0), \quad (3)$$

and obtain the first flux jump field, B_{fj} , as a function only of the volumetric specific heat and of the difference between the effective critical temperature, T^* (at the prevailing magnetic field), and the operating temperature, T_0 :

$$B_{fj} = \left[3 \mu_0 \gamma C (T^* - T_0) \right]^{0.5}. \quad (4)$$

It is worth noting that the critical current density is not explicitly present in Eq. (4), but does affect the depth of flux penetration according to Eq. (1). The higher the current density, the smaller the penetration depth and the steeper the field gradient. For subsequent flux jumps, equation (4) can be generalized by replacing B_{fj} with the difference, ΔB , between the fields inside and outside the body of the superconductor.

Fig. 3 gives the temperature variation of the first flux jump field for a "generic" High Temperature Superconductor with the appropriate physical properties, as discussed in a companion paper. [6] For materials with a T_c higher than about 90 K, the peak will increase and shift to higher temperatures. The actual magnitude and location of the peak depend strongly on the value of the specific heat and may change somewhat as new materials and more accurate data become available. The figure also shows the upper critical field, B_{c2} . Obviously, there can be neither superconductivity nor flux jumps above that line. At any rate, our model using a field-independent, constant critical current density will have to be modified for detailed studies in the vicinity of B_{c2} by assuming a more realistic constant pinning force.

Flux Jump Field & Bc2

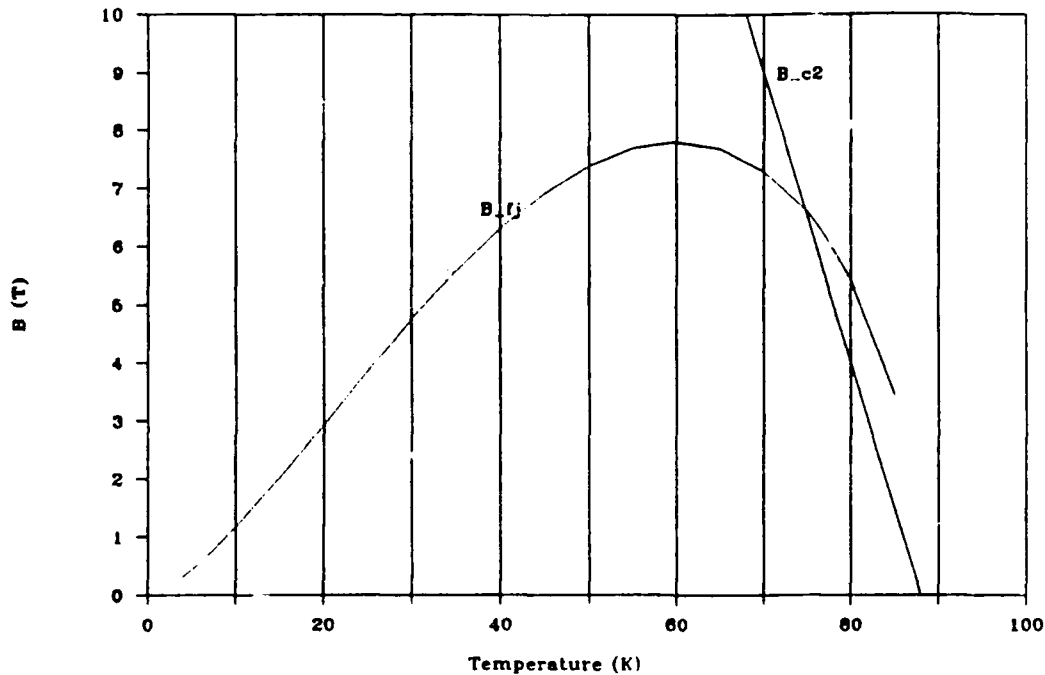
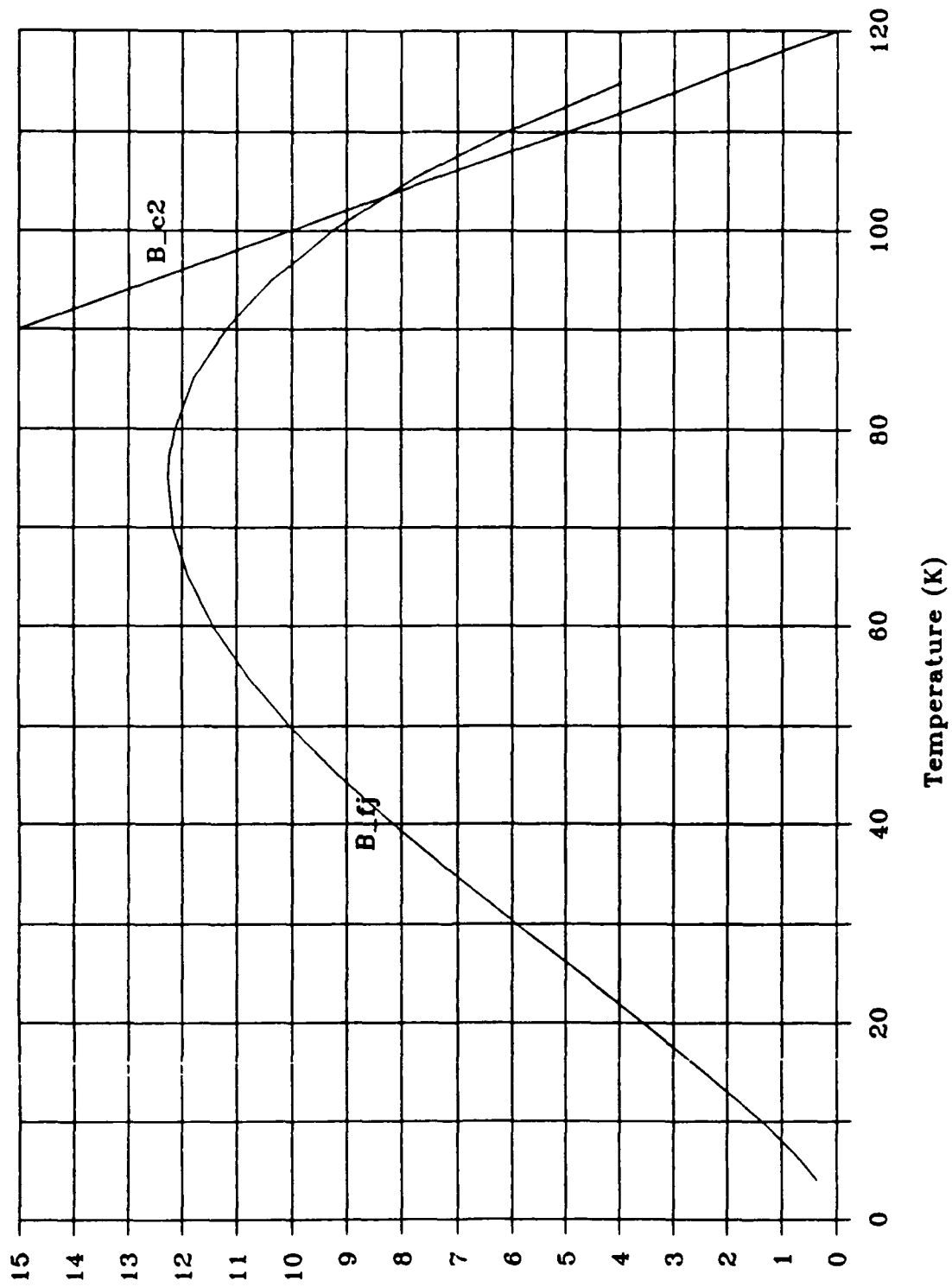


Fig. 3a Flux Jump Fields for 90 K High Temperature Superconductor as a Function of Temperature.

Fig. 3b Flux Jump Fields for 120 K Superconductor. (See Next Page)

Having established the maximum safe field difference across a bulk superconductor, we can use Eq.1 to calculate the thickness of the slab that can just support that field difference. We designate the corresponding threshold value for the half-thickness as a_{fj} . In other words, $2 \cdot a_{fj}$ is the maximum safe thickness of superconducting material that, at the operating temperature and at the prevailing critical current density, will just be penetrated (from both sides) when the externally applied field is equal to the calculated flux jump field. For circular geometries, the distance a_{fj} becomes the radius of a solid cylinder, or the wall thickness of a tube, and the numeric values of B_{fj} and a_{fj} are enhanced by about 10% over the slab values.

Flux Jump Field - 120 K Superconductor



B (T)

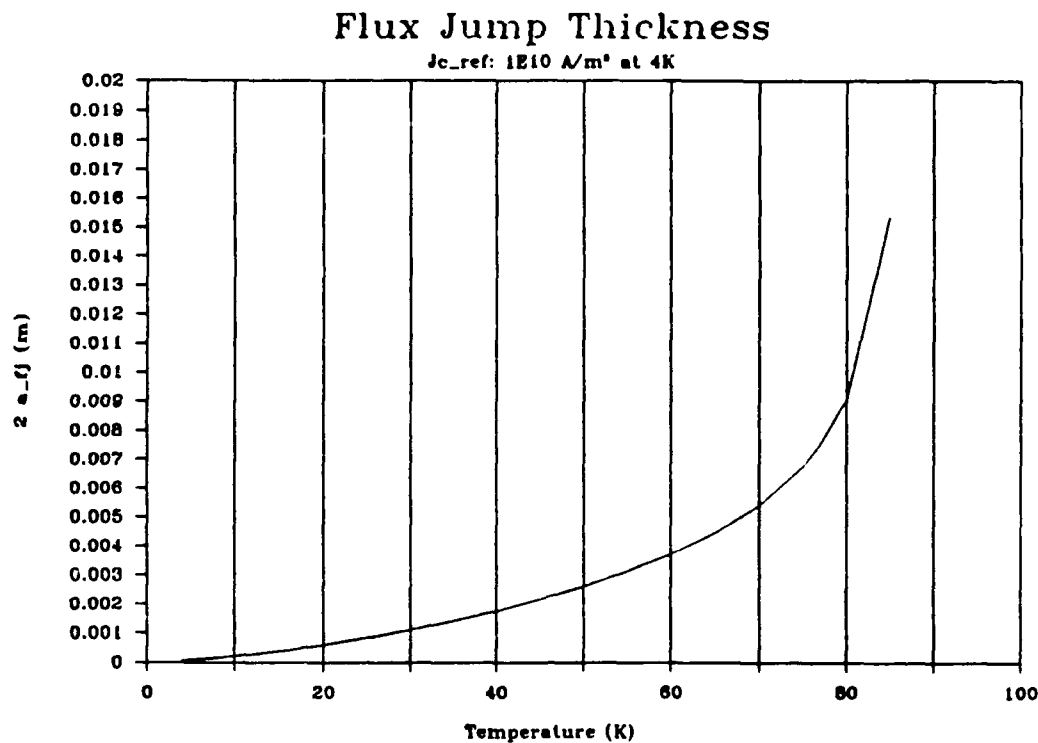


Fig. 4 Flux Jump Dimension in High Temperature Superconductor as a Function of Temperature.

Fig. 4 gives a plot of $2 \cdot a_{fj}$ as a function of temperature when the critical current density drops linearly from a reference value of 10^{10} A/m^2 at 4 K to zero at a T^* of 88 K. This corresponds to a critical current density of $1.2 \cdot 10^9 \text{ A/m}^2$ ($1.2 \cdot 10^5 \text{ A/cm}^2$) at 77 K. Since a_{fj} is inversely proportional to J_c , a 10-fold decrease in J_c will cause a 10-fold increase in a_{fj} . The data of Fig. 4 are re-plotted in Fig. 5 on a logarithmic scale.

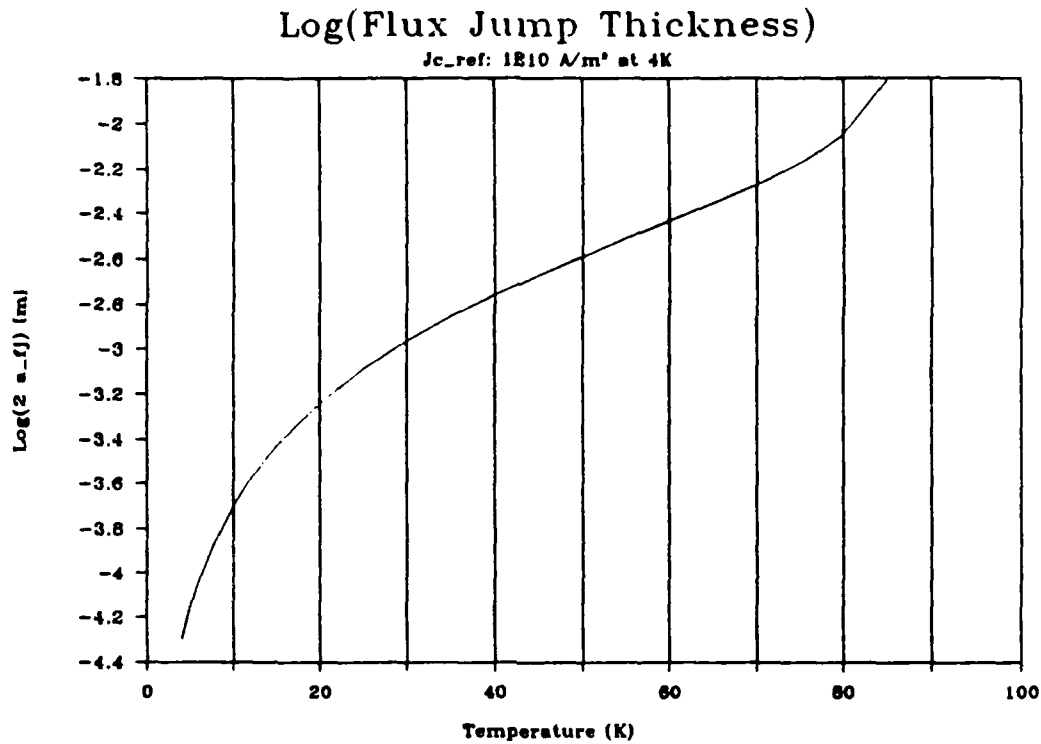


Fig. 5 *Logarithm of Flux Jump Dimension in High Temperature Superconductor as a Function of Temperature.*

3. Flux Creep

As mentioned, adiabatic conditions need not always prevail. In that case thermally activated flux creep will redistribute critical currents throughout the superconductor, as described by the Kim-Anderson model. The increased ease of flux creep at elevated temperatures will, on one hand, reduce achievable critical current densities, by making pinning sites less effective, but may, on the other hand, slow the re-distribution of flux lines sufficiently, so that the dimensional limits of the adiabatic model can be safely exceeded.

The existence of flux creep indicates that the concept of a unique value for the critical current density of a Type II superconductor is somewhat flawed. Flux creep can only be observed in persistent current systems, which are operating at their critical current density, but this is exactly where critical state flux trapping assemblages will be. Some flux will creep or leak out and the field will decay with time. Fortunately, the decay is not exponential with a single time constant, but instead it is logarithmic in time. As shown by the Kim-Anderson model, the time for a given fractional decay increases logarithmically, so that changes soon become unobservable and the fields are "constant" for all practical purposes. One way to avoid even the small initial decay and at the same time stabilize the magnet against the effects of temperature fluctuations, would be to operate at a temperature lower than the trapping temperature.

4. Flux Trapping

4.1. Superconductor Magnetization Patterns

In the following description of the magnetization behavior of superconducting slabs or structures, when subject to (cyclically) changing fields, it is convenient to normalize all fields to the penetration field, B_p , needed to push the current boundary from the surface to the center of the given geometry during the first or virgin cycle. Fig. 6 displays the phasing of the average field or induction, B_{avg} , within the semi-infinite slab and of the magnetization, M , when the externally applied field, measured in units of $\mu_0 H$, is cycled to $\pm 2B_p$.

Fig. 7. gives the corresponding magnetization curves for maximum applied fields, B_{max} , of 0.5, 1, 1.5 and $2B_p$. (Magnetization curves are usually shown in the superconductivity literature with the negative magnetization plotted in the +y direction, *i.e.* as the mirror image of Fig. 7).

Fig. 8 presents hysteresis curves for the average field or magnetic induction within the slabs for the same values of B_{max} , and Fig. 9 shows the field penetration patterns in the slab of thickness $2a_{\perp j}$, corresponding to different ballooned locations in Figures 6 and 8. It also lists the magnitude of the magnetization at these points.

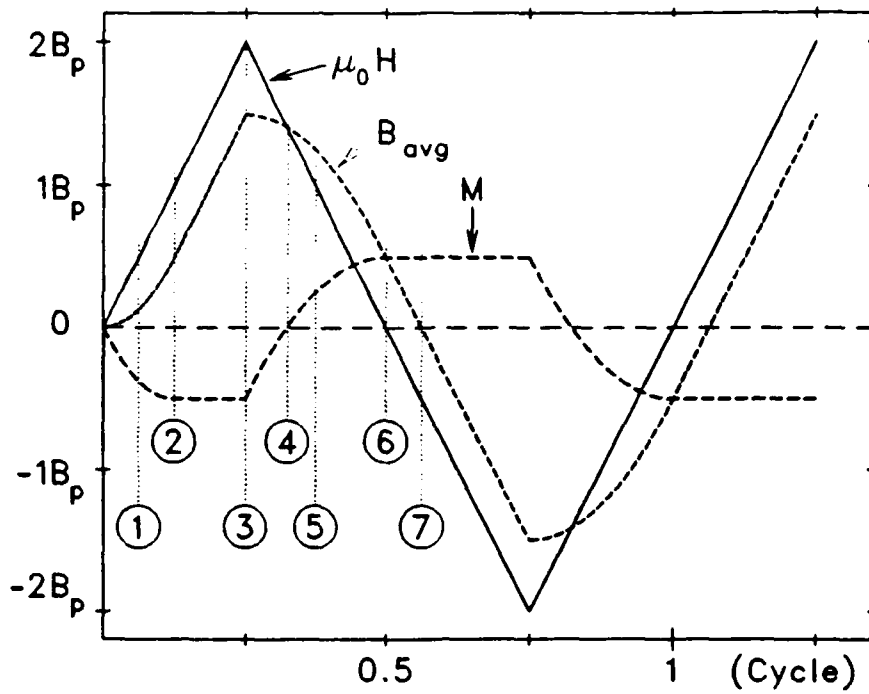


Fig. 6 Phasing of Flux Penetration and Magnetization for Superconducting Slab with Varying Applied Field.

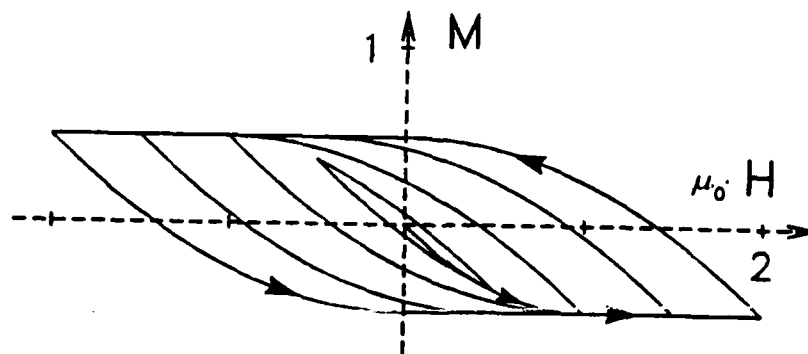


Fig. 7 Magnetization for Superconducting Slab as a Function of Applied Field. Measured in units of B_p .

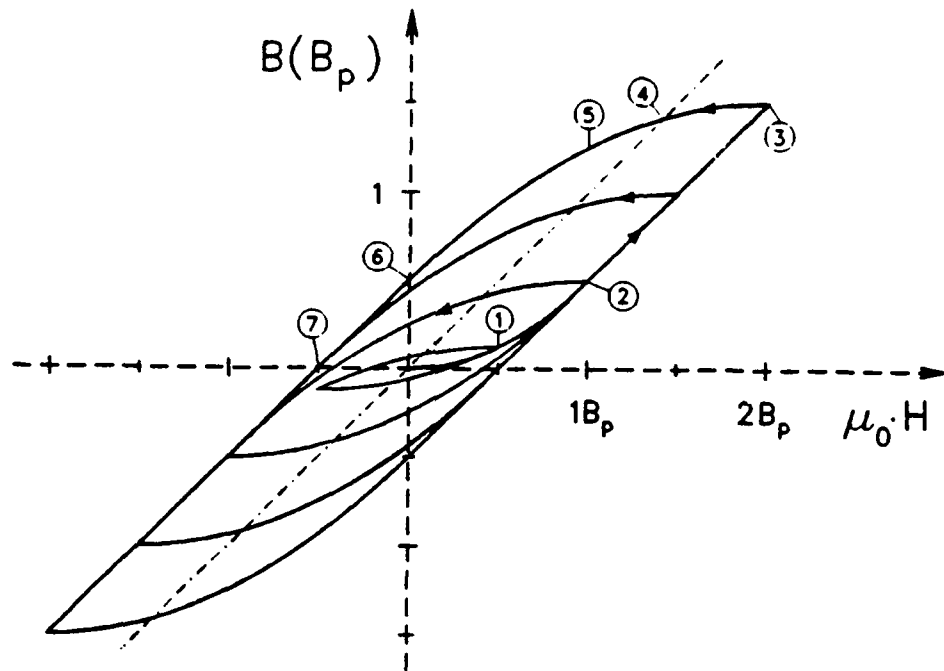


Fig. 8 Magnetic Induction Cycles in Superconducting Slab for Different Maximum Values of the Applied Field.

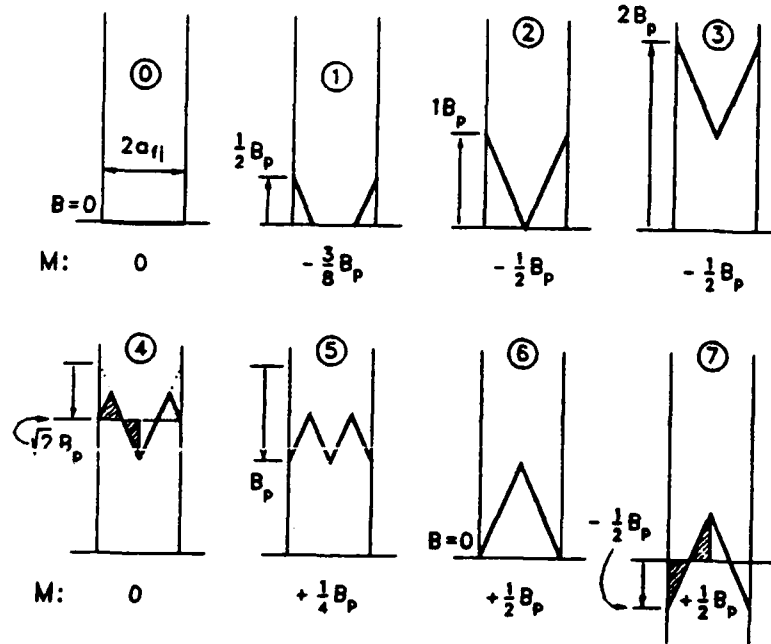


Fig. 9 Flux Penetration Patterns for Superconducting Slab and Value of Magnetization at Different Points of the Hysteresis Cycle.

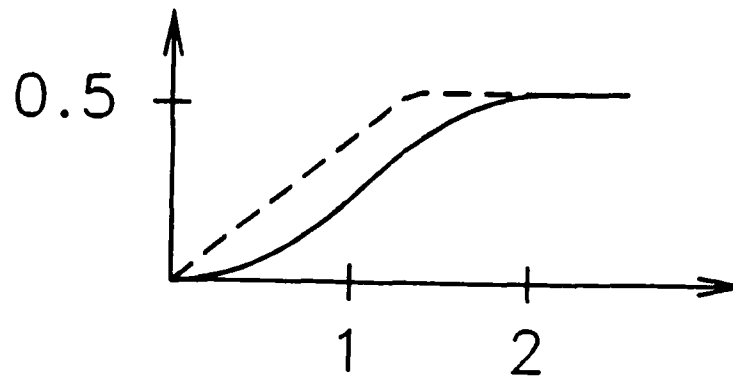


Fig. 10 Remanent and Coercive Fields for Superconductor as a Function of Maximum Field Applied During Cycle. Measured in units of B_p . Coercive field, dashed curve, drops linearly.

During the part of the cycle where the applied field is decreased, the direction of newly induced currents moving in from the surface is reversed. They now try to reduce and eventually reverse the average field within the material. After the first reversal of the sweep direction, the moving boundary is no longer between critical current and zero current density, but between critical currents of opposite direction.

It should also be noted that, with our system of coordinates, the induction curves, Fig. 8, are merely the magnetization curves, Fig. 9, sheared vertically to a 45° angle. This should not be surprising, since $B=M+\mu_0 H$. It also makes it obvious why, in Fig. 9, the zero magnetization balloon 4 falls on the 45° line. The virgin state, balloon 0, would also fall on that line, but has been omitted from figures 6 and 8 to reduce crowding. "Saturation" could be indicated by parallel 45° lines, displaced vertically by $\pm B_p/2$. Therefore, both the maximum possible remanent field, B_r at balloon 6, and the coercive field, $\mu_0 H_{c1}$ at balloon 7, are equal to $B_p/2$. Fig. 10 shows how the peak value of the magnetizing field affects the magnitude of the remanent and coercive fields. A field of $2B_p$ has to be applied to obtain the maximum possible remanence of $0.5B_p$. The coercive force drops linearly with decreasing B_{max} .

4.2. Comparison with Conventional Permanent Magnets

To compare flux trapped superconducting structures with conventional permanent magnets entails a comparison of totally different physics. There are no contributions from "atomic material currents" and all fields can, in principle, be calculated simply from the Biot-Savart law by superposing contributions from frozen-in, persistent supercurrents. There is no large permeability or inherent field enhancement, as in ferromagnetism, and μ_0 , the permeability of free space, applies throughout the superconductor.

It is not surprising, therefore, that the terminology that has evolved to describe magnetization and hysteresis in Type II superconductors differs from the corresponding usage with ferromagnetic materials. Although some of the comparisons have already been mentioned in the previous section, we summarize the similarities and differences by listing the conventional terms, as defined by Humphries. [7]

Magnetizing Force. The externally applied field, H , corresponds to the magnetizing force, or magnetic intensity, usually given in $A \cdot \text{turn/m}$ or oersteds. To simplify the analysis, our curves are plotted with $\mu_0 H$ for the abscissa.

Magnetic Induction. The average magnetic field within the perimeter of the superconductor, B_{avg} , corresponds to the (normal) magnetic induction and is, indeed, the average magnetic flux density. As seen in Fig. 6, it always lags behind the magnetizing force and its magnitude varies across the superconductor, as evident in Fig. 9.

Magnetization. The magnetization (sometimes called the intrinsic induction) is the difference between normal magnetic induction and magnetizing force, or between average field and applied field, and is initially negative for the superconductor (Fig. 6).

Remanence. The remanent field, B_r , is the field that is trapped when the external field is reduced to zero.

Saturation. Saturation for SuperPermanent magnets is indicated by the minimum value of the temporarily applied field that will leave the maximum possible value for the remanent field. It is only limited by critical current densities, dimensions, and the avoidance of flux jumps. If a magnetizing field of $2B_p$ is available, B_r will saturate at $B_p/2$.

Coercivity. In the superconducting case, we only have the normal coercivity, H_{cn} , where the normal induction curve crosses the abscissa. Coercivity and remanence cannot be modified independently of each other. The zero average field at the coercive force position is just the result of compensating persistent currents. There is no physically meaningful intrinsic coercivity for the superconductor, as should be evident from Fig. 7.

Energy Product. The energy product measures the energy stored in the magnetic structure or needed to demagnetize it. As such, it governs interactions with the outside world or the magnetic "hardness". When fully magnetized, its maximum value is $B_p^2/4\mu_0$.

Curie Point. The superconducting transition temperature, T_c , corresponds to the Curie temperature, in that the material has to be heated to that temperature to be completely demagnetized to restore the virgin state and, more importantly, be kept well below it to retain the trapped flux.

Fig. 11 sketches the behavior of conventional permanent magnet materials in a plot corresponding to Fig. 8. The narrow magnetization range for Alnico™, is distinctly different, but the curves for the modern Rare Earth - Transition Metal (RE-TM) [8] [9] permanent magnet compounds are more similar to the superconductors in terms of the extended values for both, the magnetizing and demagnetizing, fields. (There are other similarities, including complex chemistry, anisotropy and ceramic manufacture.)

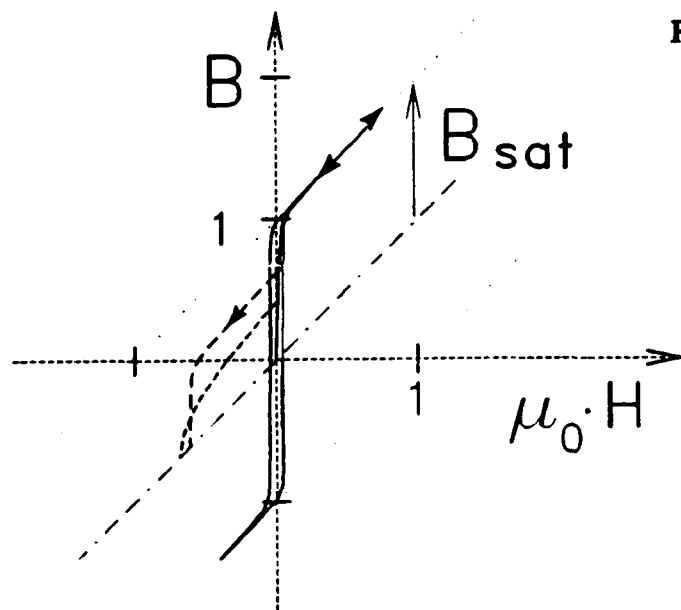


Fig. 11 Magnetic Induction for Permanent Magnets Plotted as for Superconductors in Figure 8. Fields normalized to saturation induction. Narrow solid curve is for typical Alnico™. Dashed curve with arrow is for Nd-B-Fe with a saturation $\mu_0 H$ of 2 T [8]; other dashed curve is for similar melt-spun material [9].

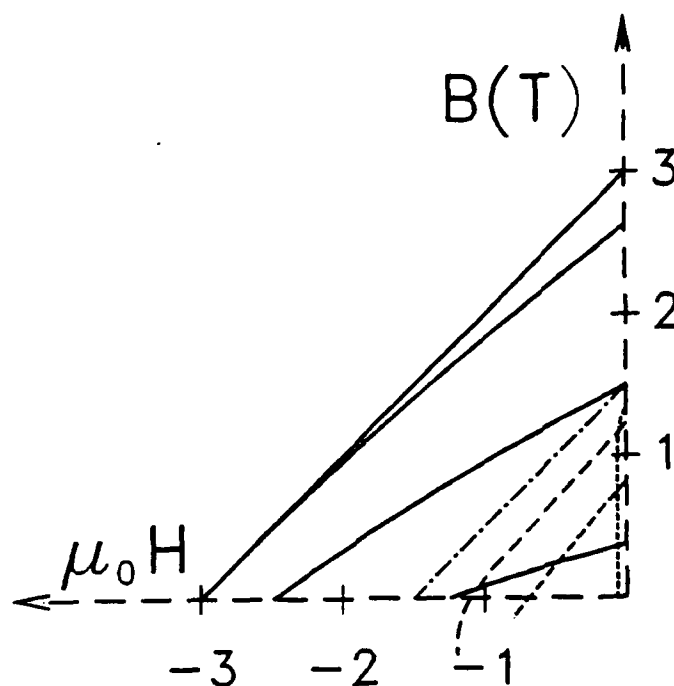


Fig. 12 Demagnetization of Superconductors and Permanent Magnets.

Actual fields are given in teslas. The solid lines are for superconductor of optimum thickness $2a_{FJ}$, magnetized to 12, 9, 6 and 3 T, respectively. The dot-dashed line is for a superconductor of only half the optimum thickness. The 45° dashed lines are for Nd-Fe-B and the steep dashed curve is for Alnico™.

5. Testing and Using SuperPermanent Magnets

The utility and performance of a given material as a permanent magnet is established by the energy product, as exhibited in the second quadrant of the induction curves. Fig. 12 enlarges the second quadrants of figures 8 and 11 and translates from normalized to actual fields. A conservative value of 6 T has been assumed for the flux jump field, as appropriate for 77 K operation, and the half-thickness a_{FJ} corresponds to full flux penetration at that field. Table I summarizes the results of our analysis by listing the energy product for various materials, configurations and magnetizing fields. It also includes some RE-TM magnets for comparison.

Table I

Energy Products

	B_{\max} (T)	MJ/m ³	MG·Oe
Full Thickness	12	1.8	225
	9	1.7	210
	6	0.8	100
	3	0.1	12
Half Thickness	6	0.45	56
Sagawa et al [8]	2	0.29	36
Croat et al [9]	2	0.11	14

It is apparent that specimens of less than full penetration thickness will not demonstrate the real potential of high temperature superconductors.

Table II gives the dimensions required to utilize the 6 T flux jump field at various critical current densities and thereby points out the major problem and weakness of the concept at the present stage of development of high temperature superconductors. Clearly, even a meter thick sample is neither practical nor desirable. However, current densities of 100 A/mm² at 77 K appear to be on the horizon, which corresponds to a more reasonable size of 10 cm. A most useful size of 1 cm would result from the long-term goal of current densities of 1000 A/mm², as was also used in Fig. 4.

Table II

Sample Dimensions

A/mm ²	J_c	$2a_{fj}$
	A/m ²	mm
2	2E6	4800
10	E7	950
100	E8	95
1000	E9	9.5

It should be emphasized that the dimensions in Table II follow from the relations between critical current densities and the critical state model and will be valid even if flux jumps turn out to be less of a problem than we have assumed.

One obvious way to test the concept and determine superconductor stability with presently available materials would be to make measurements on thin-walled cylinders or stacked washers over a range of temperatures. Higher current densities are automatically available below 77 K, albeit at the expense of reduced stability. Such configurations will also allow taking advantage of the additional possibilities that result from the anisotropy of the critical current densities, once textured materials become available.

Clearly, there are tremendous technological opportunities here, if the preceding analysis can be verified experimentally and when high temperature superconducting materials of improved current densities are available.

Conclusions

- 1) High temperature superconductors may be used as permanent magnets with trapped fields of 3 T at 77 K.
- 2) Their energy product should be as high as 1.8 MJ/m^3 or 225 MG-Oe.
- 3) The magnetizing field has to be 4 times as large as the trapped field, or 12 T.
- 4) Permanent magnet use of high temperature superconductors bypasses the problems of wire or tape manufacture.
- 5) Flux jump instabilities will be less important at 78 than at 4 K.
- 6) Widespread use of the concept will depend on improved critical current densities.

REFERENCES

- [1] H.L. Laquer, Flux trapping and flux pumping with solenoidal superconductors, *Progress in Refrigeration Science and Technology - 1963-1*, Pergamon Press, Oxford 1965, p 207-13.
- [2] C.P. Bean, Magnetization of hard superconductors, *Phys. Rev. Lett.* **8**, 250 (1962).
- [3] H. London, Alternating current losses in superconductors of the second kind, *Phys. Lett.* **6**, 162 (1963).
- [4] M.N. Wilson, C.R. Walters, J.D. Lewin and P.F. Smith, Experimental and theoretical studies of filamentary superconducting composites, *Jour. Phys. D.* **3**, 1517 (1970).
- [5] Martin N. Wilson, *Superconducting Magnets*, Clarendon Press, Oxford, 1983, 335 pp.
- [6] H.L. Laquer, F.J. Edeskuty, W.V. Hassenzahl and S.L. Wipf, Stability Projections for High Temperature Superconductors, *CryoPower Report TR-88-01*, March 1988, 22 p.
- [7] Stanley Humphries, Jr. - *Principles of Charged Particle Acceleration*, John Wiley and Sons, New York, 1984.
- [8] M. Sagawa, S. Fujimura, N. Togawa, H. Yamamoto, and Y. Matsuura, New material for permanent magnets on a base of Nd and Fe, *Jour. Appl. Phys.* **55**, 2083 (1984).
- [9] J.J. Croat, J.F. Herbst, R.W. Lee, and F.E. Pinkerton, Pr-Fe and Nd-Fe-based materials: A new class of high-performance permanent magnets, *Jour. Appl. Phys.* **55**, 2078 (1984).